

Image potential for stepped and corrugated surfaces

William L. Clinton, Mark Esrick,* Herbert Ruf, and William Sacks

Department of Physics, Georgetown University, Washington, D.C. 20057

(Received 3 July 1984)

The classical image potential is derived for a nonplanar conducting surface. A general formulation is given for first-order deformations of an arbitrary shape. Detailed formulas are presented for a variety of rectangular step and terrace configurations including corrugations. It is shown that ions and electrons are always attracted to the elevated part of the surface. Potential-energy minima and hence bound states parallel to the surface can exist on a track or terrace. Classical trajectories are calculated in some special cases and compared to the plane conductor. The effects produced by these nonplanar surfaces on ion angular distributions are also discussed.

I. INTRODUCTION

The classical image potential plays a significant role in many areas of surface physics. In any experiment or model calculation involving ions or electrons in the vicinity of a plane conductor there is a contribution to the potential of the classical image form: $V_I(z) = -q^2/4z$, where q is the charge and z is the distance to the image plane expressed in atomic units. More generally, in the case of a material with dielectric constant ϵ ,

$$V_I(z) = -\frac{\epsilon-1}{\epsilon+1} \frac{q^2}{4z},$$

as for an electron near a liquid-He surface.

Our purpose in this paper is to point out that $V_I(z)$ takes a more complicated form in the vicinity of nonplanar surfaces such as one might find for realistic materials. We refer to steps, terraces, facets, corrugations, adsorbate overlayers, and other modifications or defects in the perfectly planar surface. Specifically, we will derive a first-order expression for the change in the image potential for general surface deformations. In addition, we will give detailed results for certain well-defined surface modifications such as an infinite rectangular step, an infinite rectangular track and/or trough, and certain periodic arrays of tracks and troughs which could represent surface corrugations (see Fig. 2 for details). Before presenting these details we give a brief overview of the specific subfields where the classical image potential for plane conductors has proven to be a fruitful concept.

In low-energy ion-surface interactions such as those that occur in ion desorption arising from electrons, photons, or sputtering, the ions detected are in a sufficiently low energy range (0–40 eV) that image-potential corrections can be significant. For example, recent work by Misković, Vukanić, and Madey¹ shows how ions are distorted in unbound desorption trajectories resulting in possible large uncertainties in the interpretation of ion angular distributions. In addition, Madey² has discussed the possible interesting effects that may result in the bound trajectories of the image potential.

In the area of sputtering, Gibbs *et al.*³ have shown that the inclusion of an image potential in the classical trajectory calculations of sputtering yields leads to improved

agreement with the experimental yield data. In addition, theoretical work by Norskov and Lundqvist⁴ uses the image potential to help explain sputtering data of Yu.⁵

In the various techniques involving electron scattering from metal surfaces, the image-potential concept has generated myriad effects, some of which are as yet unobserved. For example, in low-energy electron diffraction (LEED) the image potential is responsible for a wealth of low-energy fine structure attributed to surface resonances above the vacuum level. These resonances have been studied in detail by McRae.⁶ In related work, Dietz *et al.*⁷ have interpreted high-resolution LEED fine structure for Cu(001) in terms of a two-parameter potential with an image term. Fitting the experimental line shapes using this potential leads to the conclusion that the image potential saturates to about one-half the value of the crystal inner potential.

Inelastic electron scattering also may be affected by the image potential. Thus Hall *et al.*⁸ show how the surface resonances manifest themselves in inelastic electron scattering from adsorbate molecules using electron energy-loss spectroscopy. Although there are certain effects predicted by these authors, such as molecular vibrational selection-rule breakdown, they await experimental verification.

In photoelectron spectroscopy Gadzuk⁹ discusses the role of the image potential in interpreting the adsorbate core-hole screening energies. In particular, he shows that the screening energy is just the quantum-mechanical analog of the classical image-potential level shift.

As already mentioned, the image potential has also been invoked to explain some of the phenomena involved when electrons are in the vicinity of a liquid-helium surface. Cole¹⁰ derived the surface states in detail and also discussed the interaction of the electrons and the ripplon excitation on the helium surface. Effects of the electron states bound to the He surface have also apparently been observed from the Stark splitting of the microwave absorption spectra.¹¹

In all of these observations it is evident that deformations of the plane surface of the conductor or dielectric will cause a modification of the image potential and a concomitant change in the experimental manifestations. It is our purpose here to point out that a number of poten-

tially very exciting effects such as the attraction and repulsion of charged particles by steps, tracks, and other deformations may be observable in many of the previously mentioned experiments.

In what follows we derive the electrostatic potential energy (image potential) for the system consisting of a point charge $+q$ located outside a nonplanar conducting surface, valid to first order in the surface deformation. In a more extensive report an alternative derivation, based on Hadamard's theorem,¹² as well as a method that generates the electrostatic potential to all orders, will be presented.

II. DISCUSSION

We begin with a point charge $+q$ located a distance z above the conducting plane surface coincident with the x - y plane as depicted in Fig. 1. The electrostatic energy of the system is the usual image potential $-q^2/4z$, in Gaussian units, excluding all self-energies. If the plane conducting surface is now deformed as shown in Fig. 1, the electrostatic energy changes by the amount of work δW needed to produce the deformation. The work required to displace the surface element da' , located at the point (x',y') , by $\delta h(x',y')$ in the z direction is $\delta w = F_z(x',y') \delta h(x',y')$. Here $F_z(x',y')$ is the minimum force in the z direction necessary to produce the displacement $\delta h(x',y')$. To first order in δh ,

$$\delta w = -\frac{1}{2} \delta h(x',y') \sigma_0(x',y') da' E_{0z}(x',y'),$$

where $\sigma_0(x',y')$ and $E_{0z}(x',y')$ are, respectively, the surface charge density and the z component of the electric field at the point (x',y') on the plane conducting surface. But $\sigma_0(x',y') = E_{0z}(x',y')/4\pi$ so that

$$\delta w = -\frac{\delta h}{8\pi} E_{0z}^2(x',y') da'.$$

The final result is obtained after an integration over the plane surface with respect to da' ,

$$\delta W = -\frac{1}{8\pi} \int E_{0z}^2(x',y') \delta h(x',y') da'. \quad (1)$$

The explicit expression for E_{0z} can be obtained from the electrostatic potential $\phi(\vec{r}, \vec{r}')$ due to the charge $+q$ and its image $-q$. Thus

$$E_{0z}(x',y') = -\left. \frac{\partial}{\partial z'} \phi(\vec{r}') \right|_{z'=0}, \quad (2)$$

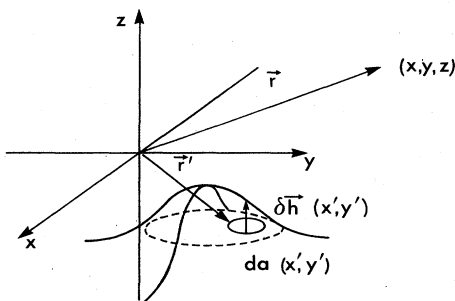


FIG. 1. Coordinate system for a general deformation of the plane surface.

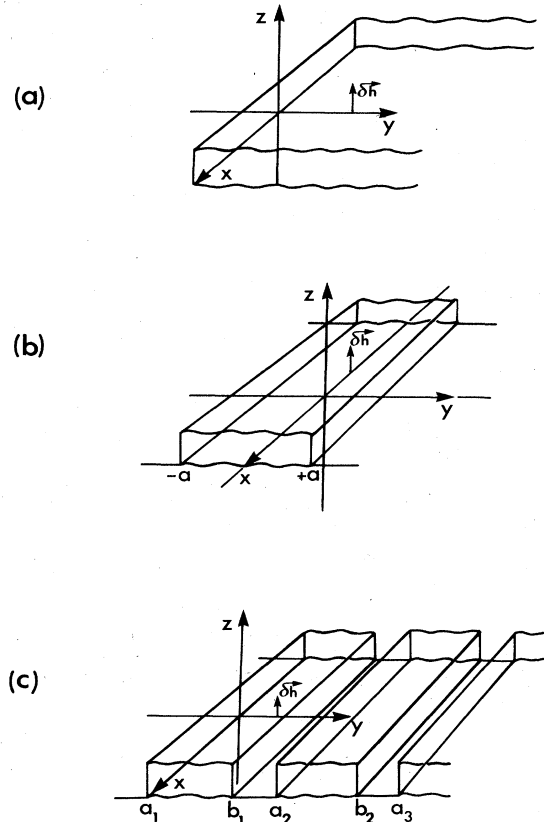


FIG. 2. Configurations for which the image potential can be determined in a simple form. (a) Infinite step, (b) infinite track, (c) rectangular corrugation.

where

$$\phi(\vec{r}, \vec{r}') = \frac{q}{[(x'-x)^2 + (y'-y)^2 + (z'-z)^2]^{1/2}} - \frac{q}{[(x'-x)^2 + (y'-y)^2 + (z'+z)^2]^{1/2}}.$$

We next consider some specific surface deformations, some of which are displayed in Fig. 2.

A. Uniformly elevated surface

As a first example, and a consistency check, we consider the trivial case of the conducting surface uniformly elevated in the z direction. Here, of course, we know the exact answer. Thus

$$\begin{aligned} W(z) &= -q^2/4(z - \delta h) \\ &= -q^2/4z \left[1 + \frac{\delta h}{z} + \dots \right] \end{aligned} \quad (3)$$

and the first-order correction is $\delta W(z) = -(q^2/4z^2)\delta h$. On the other hand, our first-order correction using Eq. (1) is given by

$$\delta W(z) = \frac{-1}{8\pi} \int_{-\infty}^{+\infty} dy' \int_{-\infty}^{+\infty} dx' |\nabla\phi(\vec{r}, \vec{r}')|_{z'=0}^2 \delta h = -\frac{\delta h z^2}{2\pi} \int_{-\infty}^{+\infty} dy' \int_{-\infty}^{+\infty} dx' \frac{q^2}{[(x'-x)^2 + (y'-y)^2 + z^2]^3} \quad (4)$$

which by elementary quadrature yields

$$\delta W(z) = -(q^2/4z^2)\delta h,$$

in agreement with the exact result.

B. Surface elevated for $y > 0$ [infinite step, Fig. 2(a)]

Here we see that the geometry dictates the following expression:

$$\delta W(x, y, z) = -\frac{\delta h z^2}{2\pi} \int_0^{\infty} dy' \int_{-\infty}^{+\infty} dx' \frac{q^2}{[(x'-x)^2 + (y'-y)^2 + z^2]^3}. \quad (5)$$

And, again by elementary methods, Eq. (5) becomes

$$\delta W(y, z) = -\frac{q^2 \delta h}{8z^2} \left[1 + \frac{y}{2(y^2 + z^2)^{3/2}} (2y^2 + 3z^2) \right]. \quad (6)$$

The first term is analogous to the correction δW given in Sec. II A above. The second term includes the y dependence and therefore is particularly characteristic of the step. This interesting result suggests that the ion is attracted to the elevated side of a step. Thus, for example, left and right steps will attract ions or electrons in opposite directions. The graphs of the potential in the y direction given in Fig. 3(a) clearly show this.¹³ Some trajectories of a charged particle in the field of the step are shown in Fig. 3(b).¹⁴ As expected, the unbound states starting from the "down side" of the step are pulled further from their original starting angle than in the case of the flat plate. Thus, for example, in electron- or

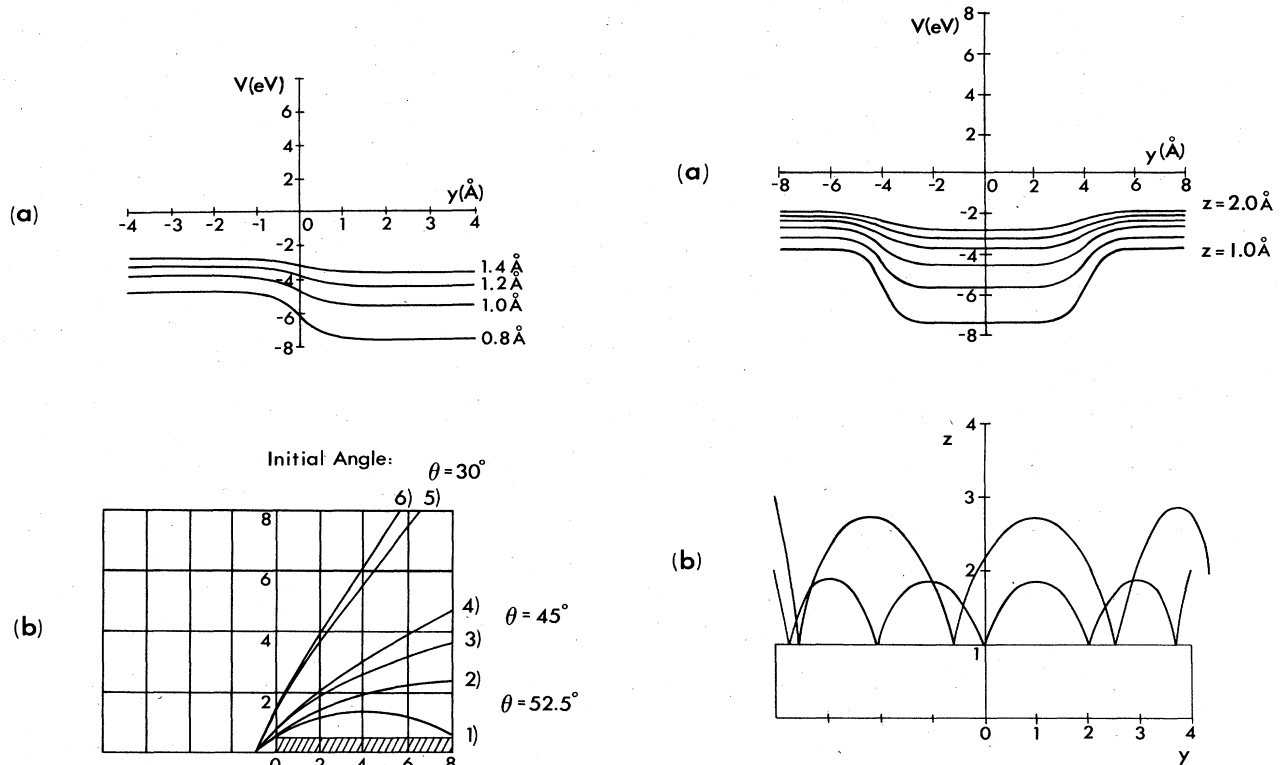


FIG. 3. (a) Image potential plotted as a function of y for various z values above a stepped surface. (b) Comparison of some bound and unbound trajectories for 0^+ desorbing a distance of 1.0 a.u. to be left of a step and having a total energy of 0.5925 a.u. (2), (4), and (6), trajectory for flat surface; (1), (3), and (5) trajectory over step of 0.5 a.u. The initial desorption angle is also shown.

FIG. 4. (a) Image potential for an infinite track of width 8 Å and height 1 Å as a function of y for various z values above the surface ranging from 1.0 to 2.0 Å in intervals of 0.2 Å. (b) Trajectories for an ion above an infinite track can be bound both in the y and z directions. Particles are dropped from a height of 2 and 3 a.u. above the left edge of the track. The end point of the trajectory near the right edge marks a reversal of the velocity in the y direction and hence the bound nature of the orbit.

photon-stimulated desorbed ion angular distributions (ESDIAD and PSDIAD), as discussed by Madey and co-workers,^{1,2} the conclusions about detection angle and initial-state bond angle are further complicated by step and surface structures. On the other hand, a detailed analysis of the ion angular distribution data could well lead to useful structural information not only about chemisorption bond angles, but also about steps on surfaces.¹⁵

C. Surface elevated for $a < y < b$ [infinite track, Fig. 2(b)]

Here the geometry dictates that

$$\begin{aligned} \delta W(y,z) &= -\frac{\delta h z^2}{2\pi} \int_a^b dy' \int_{-\infty}^{+\infty} dx' \frac{q^2}{[(x'-x)^2 + (y'-y)^2 + z^2]^3} \\ &= \frac{-q^2 \delta h}{16z^2} \left[\frac{(b-y)}{[z^2 + (y-b)^2]^{3/2}} [2(y-b)^2 + 3z^2] + \frac{(y-a)}{[z^2 + (y-a)^2]^{3/2}} [2(y-a)^2 + 3z^2] \right] \end{aligned} \quad (7)$$

for $a > 0$ and $b > 0$.

Equation (7) is plotted in the y direction and shown in Fig. 4(a).¹⁶ Here we see the interesting result that the track exerts an attractive force on the charged particles in both directions. Thus one sees the possibility of binding the charge in the y direction, i.e., the top of a conducting track is a stable channel for charged particle motion. Such a trajectory, for example, is shown in Fig. 4(b).¹⁷ This path would not be stable in the vicinity of a step since the potential energy has no minimum in the y direction.

D. Surface elevated for $a_n < y < b_n$: $n = 1, \dots$ [rectangular corrugation, Fig. 2(c)]

As indicated in Fig. 2(c), this is a periodic array of infinite tracks. Using Eq. (7) again, we now find that

$$\begin{aligned} \delta W(y,z) &= \sum_n \frac{-\delta h z^2}{2\pi} \int_{a_n}^{b_n} dy' \int_{-\infty}^{+\infty} dx' \frac{q^2}{[(x'-x)^2 + (y'-y)^2 + z^2]^3} \\ &= \sum_n \frac{-q^2 \delta h}{16z^2} \left[\frac{(b_n - y)}{[z^2 + (y - b_n)^2]^{3/2}} [2(y - b_n)^2 + 3z^2] + \frac{(y - a_n)}{[z^2 + (y - a_n)^2]^{3/2}} [2(y - a_n)^2 + 3z^2] \right], \end{aligned} \quad (8)$$

where $a_n - b_n = \alpha$ and $a_n - a_{n-1} = \beta$ serves to define the periodic nature of this configuration. If $\beta \gg \delta h$, then one just sees a periodic array of terms as in Eq. (7) and the potential is just a periodic replica of the potential in Fig. 4(a).

III. CONCLUSIONS

In summary, we have solved the problem of a point charge in the field of a nonplanar conductor deriving the image potential to first order in the height of the deformation of the surface. For various rectangular modifications of the plane surface, such as steps, tracks, and corrugations, the image potential is expressible in simple form. Since steps attract particles in the direction of the surface elevation and tracks provide channels of stable motion parallel to the surface, these results suggest the possibility of using such configurations to guide ions or electrons in near-surface trajectories.

It is also evident that steps, tracks, corrugations, and other such surface defects or structures will have interesting manifestations in the ion angular distributions of Madey and co-workers.^{1,2} Consider, for example, an atom bound to a corrugated metal surface; the spot patterns observed in the ESDIAD and PSDIAD work should be narrowed or broadened, for example, depending on whether the ion is desorbing from a crest or trough position of the corrugation. Another example is asymmetric distortion of the spot pattern when an ion desorbs from either side of a step.

Another potentially interesting aspect of the image po-

tential for nonplanar surfaces is the fact that ions and electrons will be accelerated by surface protrusions relative to the plane. It is possible, for example, that structures can be fabricated that will cause charged particles to move in various interesting periodic orbits. Thus a charged particle beam directed parallel to a metal with a fabricated corrugation will experience periodic accelerations and thus will radiate.

There are some other areas where the present results may be at least qualitatively useful. For example, in crystal growth and surface diffusion the general nature of the interaction of an atom with a step or other kind of surface deformation is obviously very important. Also, since the work function of an electron at a metal surface is a function of the surface-electron potential, any deformation tending to increase the image potential, i.e., an upward step or terrace, will increase the attraction of the electron and hence the work function. The change in work function produced by such deformations can be calculated using the methods described in this report.

We also note that although we treat only the classical image potential, the quantum calculations of, for example, Appelbaum and Hamann¹⁸ on the interaction of a static point charge with a plane surface of jellium can be modified using our results for deforming the plane jellium sur-

face and the potential used in a perturbative scheme. Such methods may have a direct application in recent experimental data such as, for example, the broadening reported by Kevan¹⁹ in angle-resolved photoemission on Cu(111) and, in addition, observations of image-potential-induced surface states^{20,21} by inverse photoemission in which detailed knowledge of the effect of the surface structure is relevant.

Finally, of current interest is the dynamical image potential such as the contributions of²²⁻²⁵ for the plane sur-

face jellium. Rahman and Maradudin²⁶ have discussed the effect of surface roughness, and surface corrugations,²⁷ on the image potential for a dielectric vacuum boundary. We are in the process of applying our results to a number of the aforementioned areas.

ACKNOWLEDGMENT

This work was supported by National Science Foundation Grant No. DMR-80-16665.

*Permanent address: Loyola College, Baltimore, MD 21210.

¹Z. Misković, J. Vukanić, and T. E. Madey, *Surf. Sci.* **141**, 285 (1984).

²T. E. Madey, in *Inelastic Particle-Surface Collisions*, Vol. 17 of *Springer Series in Chemical Physics*, edited by W. Heiland and E. Toglauer (Springer, Heidelberg, 1981), p. 801.

³R. A. Gibbs, S. P. Hollard, K. E. Foley, B. J. Garrison, and N. Winograd, *Phys. Rev. B* **24**, 7178 (1981).

⁴J. K. Norskov and B. I. Lundqvist, *Phys. Rev. B* **19**, 5661 (1979).

⁵M. Yu, *Phys. Rev. Lett.* **40**, 574 (1978).

⁶E. G. McRae, *Rev. Mod. Phys.* **51**, 541 (1979).

⁷R. E. Dietz, E. G. McRae, and R. L. Campbell, *Phys. Rev. Lett.* **45**, 1280 (1980).

⁸B. M. Hall, S. Y. Tong, and D. L. Mills, *Phys. Rev. Lett.* **50**, 1277 (1983).

⁹J. W. Gadzuk, *Phys. Rev. B* **14**, 2267 (1978).

¹⁰M. W. Cole, *Rev. Mod. Phys.* **46**, 451 (1974).

¹¹C. C. Grimes and T. R. Brown, *Phys. Rev. Lett.* **32**, 280 (1974).

¹²M. Shiffer, in *Modern Mathematics for the Engineer*, edited by E. F. Beckenbach (McGraw-Hill, New York, 1956).

¹³The image potential as given by Eq. (6) is plotted against the distance in the y direction, for a step of 0.5 Å, for various heights (z) above the stepped surface. The particle is of unit charge. For all ion trajectories, the image plane is translated a distance $z_0 = 1.62$ Å, so as to appropriately screen the image potential. A hard-wall potential is assumed at $z = 0$.

¹⁴The trajectory is calculated numerically using the Runge-Kutta method for solving simultaneous differential equations. The orbits shown are calculated for a particle of unit charge and of atomic mass 16. The initial position is 1 a.u. to the left of a step of height 0.5 a.u. and whose total energy is fixed at 8 eV. The initial angle is the angle the velocity vector makes with the z axis in the y - z plane. The trajectory over the step for various initial angles is compared to those for the flat plate. Our orbits for the flat plate, as calculated numerically,

agree exactly with those obtained by Misković *et al.* (Ref. 1) analytically. At the angle of 45° the orbit over the step is no longer critically bound, as is the case for the flat plate; rather, it is pulled in towards the plate.

¹⁵W. L. Clinton, M. Esrick, and W. Sacks (unpublished).

¹⁶Analogous to Fig. 3(a) the image potential for a track of height 1 Å and width 8 Å is plotted for the heights 1.0 to 2.0 Å above the surface.

¹⁷Trajectories are calculated for a particle whose initial velocity is zero and whose initial position is 2 and 3 a.u. above the left edge of the track. In both cases the particle is bound in the z and y direction. The end point of the trajectory near the right edge of the track is where the y component of the velocity changes sign. These need not be at the distance $y = 4$ a.u. The particle dropped at 2 a.u. has a symmetric orbit on the top of the track such that its velocity at its position at $y = 4$ a.u. is zero. Also, Fig. 4(b) indicates that the ion released at 3 a.u. does not have a symmetric orbit and still has a small velocity at $y = 4$ a.u. Its velocity in the y direction changes at about 0.5 a.u. to the right of the track. Note that particles released above a flat plate will simply bounce up and down and not be displaced in the y direction.

¹⁸J. A. Appelbaum and D. R. Hamann, *Phys. Rev. B* **6**, 1122 (1972).

¹⁹S. D. Kevan, *Phys. Rev. Lett.* **50**, 526 (1983).

²⁰D. Straub and F. J. Himpsel, *Phys. Rev. Lett.* **52**, 1922 (1984).

²¹V. Dose, W. Altmann, A. Goldmann, V. Kolac, and J. Rogozik, *Phys. Rev. Lett.* **52**, 1919 (1984).

²²P. J. Feibelman, C. B. Duke, and A. Bagchi, *Phys. Rev. B* **5**, 2436 (1972).

²³R. Ray and G. D. Mahan, *Phys. Lett.* **42A**, 301 (1972).

²⁴J. C. Inkson, *J. Phys. F* **3**, 2143 (1973).

²⁵J. R. Manson and R. H. Ritchie, *Phys. Rev. B* **24**, 4867 (1981).

²⁶T. S. Rahman and A. A. Maradudin, *Phys. Rev. B* **21**, 504 (1980).

²⁷N. E. Glass, A. A. Maradudin, and V. Celli, *Phys. Rev. B* **26**, 5357 (1982).